Available online at www.sciencedirect.com
SCIENCE DIRECT
Journal of Molecular Catalysis A: Chemical 243 (2006) 17–23
JOURNAL OF MOLECULAR CATALYSIS A: CHEMICAL
www.elsevier.com/locate/molcata

A comparative study on the structural and catalytic properties of zeolites type ZSM-5, mordenite, Beta and MCM-41

R. Dimitrova [a,*], G. Gündüz [b], M. Spassova [a]

[a] *Department of Chemical Engineering, Ege University, Bornova, Izmir, Turkey*
[b] *Institute of Organic Chemistry, Bulgarian Academy of Sciences, 1113 Sofia, Bulgaria*

Received 31 May 2005; received in revised form 11 August 2005; accepted 11 August 2005
Available online 5 October 2005

Abstract

Zeolites of different structures and textural mesoporosity (ZSM-5, mordenite, Beta and MCM-41) were investigated as catalysts in liquid phase isomerization of alpha-pinene at 373 K and in methanol conversion. The morphological characterization of the samples was fulfilled before and after the reaction by XRD, SEM, BET and temperature programmed desorption of ammonia.

Keywords: Zeolites; Mesopores; α-Pinene isomerization; Methanol conversion

1. Introduction

The technological application of zeolites is based upon the behavior of hydrocarbons within their framework structure and is governed by two factors: the zeolite acid strength and the pore size. It is well known that the former factor is related to both the Brönsted acid sites (catalyst protonation ability) and the bridging hydroxyl groups (the present aluminum ions). A correlation has been proved between the acidity of sites and the aluminum content, as the greatest acidity is achieved by zeolites with relatively low aluminium content. Besides, it was found that zeolite acidity reaches an optimum value at given aluminium content for some zeolite types [1–3]. This value depends on the procedure used for zeolite preparation and activation [4,5]. In this paper, the aforementioned effects are examined on a series of ZSM-5, mordenite, Beta and MCM-41 molecular sieves. The relative weight of factors, such as the pores size, the framework irregularities, and the strength of the Brønsted sites has been evaluated by comparative catalytic studies [6]. The acid catalysed conversion of methanol to hydrocarbons and the isomerization of the bulky alpha-pinene molecule are studied. The isomerization of alpha-pinene yields a complex mixture of monoterpenes, bi- and tricyclic products in parallel irreversible steps and it is established that the reaction could be applied as a model for determination of the acid-base properties of various solid catalysts [7–10] and zeolites [11–13]. In view of the differences reported on the zeolites' catalytic behavior, we tried to follow the role of zeolite structural disorder and mesoporosity on the nature and distribution of the catalytic acidic sites. Thus, by controlling the catalysts properties the reaction of alpha-pinene isomerization has been carried out either to camphoric (a valuable product used in the pharmaceutical industry), or to bulky hydrocarbons (used in production of polymeric compounds).

2. Experimental

2.1. Materials and characterization

The investigated H-forms of the samples were prepared from commercially available ZSM-5(90) (SudChemie) and mordenite (Leuna) as well as from those synthesized in hydrothermal conditions ZSM-5(27), Beta and MCM-41 [3,14]. The amorphous silica–alumina type "Houdry" with SiO_2:Al_2O_3 ratio of 10 was also used for comparison. The morphological characterization of the samples was performed before and after the reaction by various methods. XRD studies were done on a Philips PW 1840 diffractometer, equipped with a PW 1830 generator. The SEM microphotographs were taken on Philips XL 30S-model

* Corresponding author. Fax: +359 2 8700225.
E-mail address: zeolab@orgchm.bas.bg (R. Dimitrova).

1381-1169/$ – see front matter © 2005 Elsevier B.V. All rights reserved.
doi:10.1016/j.molcata.2005.08.015

scanning electron microscope. The surface areas and the pore volumes of the samples were obtained from the nitrogen adsorption isotherms measured at 77 K in a static volumetric apparatus (Coulter Omnisorp l00CX) up to $P/P_0 \sim 95$. Nitrogen adsorption data were evaluated as the monolayer surface area and half width of pores were calculated by using Langmuir and Dubinin-Astakhov (D-A) methods. Sample acidity was determined by temperature programmed desorption of ammonia (TPDA) in a conventional flow reactor supplied with a thermal conductivity detector.

2.2. Catalytic tests

The alpha-pinene isomerization was carried out at atmospheric pressure with 0.5 g of catalyst and 25 ml of alpha-pinene (Acros) at 100 °C under a nitrogen atmosphere. Samples were taken periodically during the course of the reaction and analyzed with a gas chromatograph (Hewlett-Packard 5980/2 with 25 m and 0.32 mm id. HP-FFAP capillary column) equipped with flame ionization detector (FID). Temperature programming (increase at a rate of 2 °C/min from 333 to 403 K and onwards at a rate 3 °C/min until 500 K) was applied for separation at l ml/min N_2 flow.

The methanol catalytic experiments were perfomed in a fixed bed reactor at atmospheric pressure. The catalysts (0.1 g) with particle size of 0.2–0.8 nm was diluted with a three-fold amount of glass. The methanol conversion was studied in a temperature range from 400 to 800 K, a methanol partial pressure of 1.57 kPa and argon used as a carrier gas. The on-line gas chromatographic analysis was done on 2 m Porapak Q and 2 m Durapak columns. The products yields were calculated using an absolute carbon base calibration.

2.3. Quantum-chemical calculations

The semi-empirical method INDO had been applied for evaluation of catalysts performance, based on the knowledge of the reactive site. A cluster approximation of a proton zeolite site was used for the computation and the evaluation of the transition state geometry and sorption energy of the intermediate state. The series of computation involve: (A) 124 atom fragment of the zeolites with its specific T-sites. The 124 atom cluster of ZSM-5 is represented with one coordinatively unsaturated T-aluminium atom; the Beta zeolite cluster is depicted with two coordinatively unsaturated T-aluminium atoms and for the MCM-41 three OH groups are coordinated to the T-aluminium atom. (B) A cluster of 41–45 atoms cut from the 124-atom cluster saturated with hydrogen atoms. The geometry of the smaller clusters did not produce great divergences of the T–O–Si bonds angles and T–O or Si–O bond distances. So, we considered it a sufficiently large fragment of the infinite crystal. The dangling bonds were saturated with hydrogen atoms, as shown on Fig. 4(C) Clusters comprising alpha-pinene attached to a cluster acid center. The relative energies of the optimized geometry, the charge of the attached carbon atom and the environmental acidic oxygen atoms have been derived and are presented in Table 6.

3. Results and discussion

XRD patterns and SEM microphotographs of the samples show that growth and crystallinity were satisfactory and in accordance with the literature data. Slight variation in the intensity of the commercial and synthesized ZSM-5 samples at $2\theta \approx 23$ were observed (Fig. 1A), most probably due to the particles shape (Fig. 2A). The observed dislocation of the XRD peaks for the pure silica MCM-41 (Fig. 1B, line 1) and the Al-doped MCM-41 gave evidence for the existence of tetrahedral aluminium (Fig. 1B, line 2) [15].

The scanning electron microscopy revealed that the synthesized ZSM-5 particles were spherical in shape with dimensions about 700 nm, whereas the commercial ZSM-5 had particles with sponge structure with dimensions less than 100 nm (Fig. 2A and B). According to the SEM data the micrographs of the Beta zeolites display ball-like discrete particles in the range of 100 nm. There are obviously not single Beta monocrystals but clusters of spherical particles.

Physicochemical characteristics of the samples differ significantly as it was seen form the data presented in Table 1. The values for the BET surface areas and total acidity were in agreement with the literature data. The total acidity was less for samples with greater amorphisation (MCM-41, Beta) in comparison with the well crystallized ones (ZSM-5 and mordenite). It should be noted that we found low Lewis/Brønsted ratio (0.4–0.7) for the samples, determined from the the integral intensity of the band at 1455 cm^{-1} for the Lewis acidity and from the integral intensity of the band at 1546 cm^{-1} for the Brønsted acidity in the IR spectrum of adsorbed pyridine.

Major divergences were observed for the values of samples total pore volume above 1 nm. For MCM-41, ZSM-5(90) and Beta(55) the percent of the pores between 10 and 20 nm was predominant. The external surface areas (meso-macro pores) were also found to be the greatest for Beta(55) and MCM-41 samples. The differences of the physicochemical characteristic were perceived in the catalysis.

The average sample pore width was large enough to allow methanol diffusion, so its conversion was expected to reveal the nature of the acid centres. The mechanism of methanol decomposition involves the formation of surface methoxy groups, as a first step, which was more or less stable. The stability of these groups depends on the strength of the Brønsted acid sites. The sorbed carbon atom interacts by nucleophilic attack at the methyl group of a second methanol molecule, leaving water coordinated to the framework defect site. Thus, the defects in the vicinity of the Brønsted acid center have a major influence on methanol conversion. It was shown that the reaction course depended on the samples total acidity (Fig. 3). For comparison the methanol conversion over amorphous silica–alumina (Fig. 3, line 5) is shown as well.

On Beta(20) and MOR(23), the methanol conversion began at about 425 K and reached high values (98–75 wt.%, respectively) with a temperature increase of about 150 K (Fig. 3, lines 1 and 2). The dimethylether (DME) was the only observed product, proving the existence of strong Brønsted sites. At temperatures

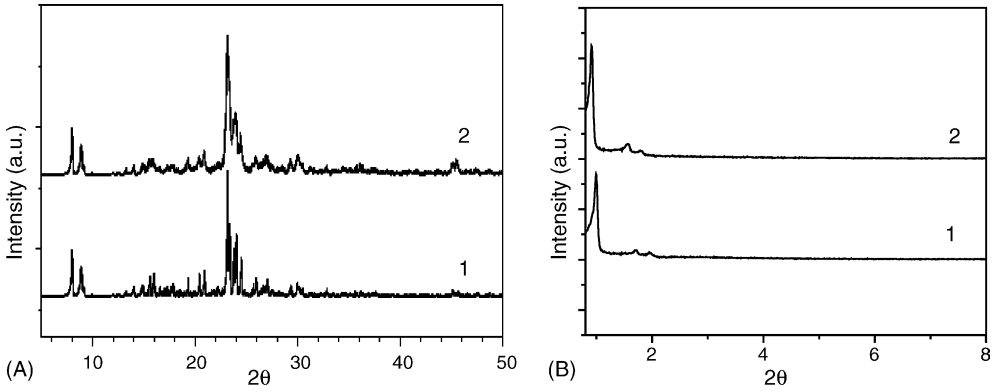

Fig. 1. XRD patterns: (A) ZSM-5(27)—line 1 and ZSM-5(90)—line 2; (B) MCM-41—line 1 and MCM-41(24)—line 2.

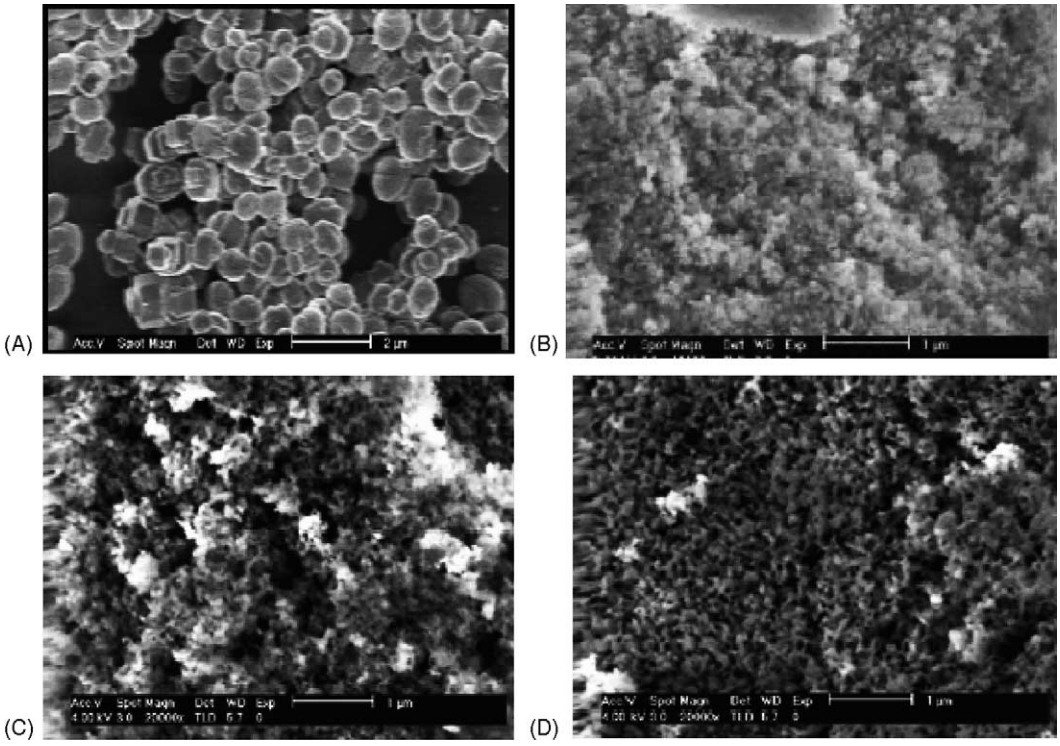

Fig. 2. SEM pictures of: (A) ZSM-5(27); (B) ZSM-5(90); (C) Beta(20); (D) MCM-41.

Table 1
Catalysts characteristics

Sample[a]	BET[b] (m^2/g)	Desorbed ammonia (mmol/g)	Total pore volume >1 nm (cm^3/g)	% of pores between			Aext (*t*-plot) (m^2/g)
				5 and 10 nm	10 and 20 nm	20 and 30 nm	
ZSM-5(27)	469.1	0.88	0.0357	22	9	5	64.37
ZSM-5(90) (commercial)	467.2	1.21	0.3761	25	43	22	114.49
MOR(23)	288.9	1.50	0.0201	24	19	8	16.86
Beta(20)	400.7	1.00	0.0632	17	25	37	43.3
Beta(55)[c]	612.9	0.86	0.7431	22	52	7	227.7
MCM-41	1030.8	0.50	0.1338	10	27	10	1542.1
MCM-41(24)	772.2	1.01	0.4349	24	28	4	701.44

[a] The number in the brackets shows the SiO_2/Al_2O_3 ratio.
[b] At $P/P_o = 0.983$.
[c] Calcined at 823 K in an oven before transformed in hydrogen form.

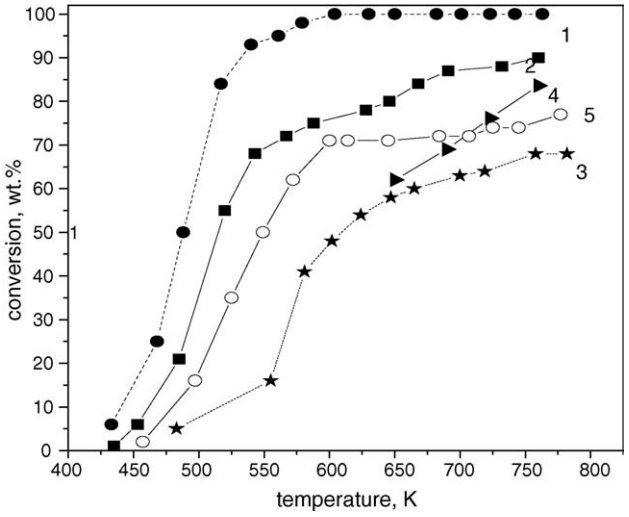

Fig. 3. Conversion of methanol over: Beta(20)—line 1; MOR(23)—line 2; ZSM-5(27)—line 3; MCM-41(24)—line 4; amorphous—line 5; range of 400–800 K.

above 500 K, light olefins were identified in the reaction product over all samples. A considerable increase in methane production in the order Beta(20) < MOR(27) < ZSM-5(27) < MCM-41(24) at temperatures above 600 K was also observed. It had been concluded that the decrease of the amount of strong Brønsted sites (due to coke formation) and the framework disorder, due to the alumina and silica tetrahedral arrangement, seemed to be a factor in methane or olefin formation.

As the MCM-41 structure was known to be of significant disorder, comparative experiments had been carried out with amorphous silica–alumina. The similarity in the acidic sites of the amorphous silica–alumina and of the molecular sieves of MCM-41 type has been previously described in [16]. Table 2 shows the product distribution at high temperatures (660–760 K) for both catalysts. The conversion of methanol catalyzed by MCM-41 began at temperatures above 660 K and significant yields of methane and olefins were identified as reaction products. DME was the main product in the entire temperature range in presence of the amorphous sample. Thus, the alumina–silica tetrahedral arrangement and consequently the acid site distribution were necessary factors in the methane or alkene formation from methanol.

Table 2
Methanol conversion on MCM-41 and amorphous silica–alumina

Sample	T (K)	Products yields (mol%)		
		CH4	C2–C5	DME
MCM-41(24)	665	21.64	21.16	48.11
	723	28.00	25.22	46.73
	760	37.00	18.13	45.00
Amorphous silica–alumina	690	11.82	–	88.00
	723	11.00	–	89.00
	760	12.00	–	88.00

The site-access restriction should play an important role in addition to zeolite framework defects and acidity in alpha-pinene isomerization, as it is a larger molecule (144.8 A^3) than methanol. The data of alpha-pinene total conversion (X_α) at a reaction temperature of 373 K and a catalyst loading of 42.9 (defined as g alpha-pinene/g catalyst) are compared in Table 3.

As seen in the Table, sample activity was in an order: Beta(55) > MCM-41(24) > ZSM-5(90) > Beta(20) > MCM-41 > ZSM-5(27) > MOR(23). An increase of alpha-pinene conversion was shown to occur in presence of zeolites with an increasing SiO_2/Al_2O_3 ratio (ZSM-5(27) and ZSM-5(90), or Beta(20) and Beta(55)). An explanations of this effect could be due to: (i) an increase in the hydrophobicity of the samples at higher SiO_2/Al_2O_3 ratios, causing high adsorption of alpha-pinene; and (ii) existence of low number but stronger acid sites per gram of zeolite (based upon the desorbed NH_3 measurements given in Table 1). Acidic sites exist on the external surface of the catalysts where the isomerization could take place as well. Thus, the low conversion of alpha-pinene over samples ZSM-5(27), MOR(23) and Beta(20) could be related to their low external surface areas (Table 1). The low conversion registered in presence of MCM-41, despite its large external area, is related to its low total acidity. A conversion of about 100% was observed in presence of sample Beta(55), which possessed an appropriate combination of strong acidity (about 0.9 mmol/g) and high percentage of wide pores (about 52% of pores between 10 and 20 nm). The presence of wide pores, however, favored the formation of limonene, terpinenes and terpinolenes. Furthermore, heavy products were obtained from

Table 3
Alpha-pinene conversion (X_α), product yields (%) and selectivity at 373 K

Sample	X_α	Camphene yield	Limonene yield	Camphene selectivity	Limonene selectivity	Selectivity ratio of camphene/(camphene + limonene)
ZSM-5(27)	1.8	0.015	–	0.80	–	100
ZSM-5(90)	14.5	3.53	0.41	24.32	2.83	89.58
MOR(23)	0.4	0.04	–	9.98	–	100
Beta(20)	6.6	2.69	2.435	41.03	37.1	52.52
Beta(55)	99.24	26.78	–	26.99	–	100
MCM-41	2.9	0.76	–	26.35	–	100
MCM-41(24)	44.7	19.797	17.04	44.25	38.09	53.74
Amorphous silica–alumina	73.9	29.40	25.36	39.79	34.32	53.69

Table 4
Reaction products (wt.%) after 3 h

Sample	LRTP[a]	Alpha-pinene	Camphene	α-Terpinene	*p*-Cymene	Limonene	α-Terpinolene	*i*-Terpinolene	Terpinden	UP[b]	HRTP[c]
ZSM-5(27)	–	96.49	0.24	–	–	–	–	–	0.38	–	2.90
ZSM-5(90)	0.6	84.04	4.10	4.31	0.71	0.40	0.24	–	–	5.59	–
MOR(23)	–	99.37	0.28	–	–	–	–	–	–	–	0.35
Beta(20)	–	93.07	3.08	–	–	2.43	–	–	0.44	0.99	–
Beta(55)	8.16	0.74	27.58	9.60	5.94	–	3.77	0.44	5.25	6.81	31.71
MCM-41	–	85.88	2.14	–	0.62	1.76	–	0.38	–	3.2	6.02
MCM-41(24)	–	53.17	20.81	1.04	3.73	16.65	0.71	–	–	3.11	0.78
Amorphous silica–alumina	0.54	25.26	30.11	3.31	7.28	24.73	0.81	–	–	5.75	2.21

[a] Products with a retention time lower than alpha-pinene (low retention time products).
[b] Products with a retention time in the range between alpha-pinene and terpinolene (unidentified products).
[c] Products with a retention time higher than terpinolene (high retention time products).

disproportionation of terpinenes or terpinolenes. Recycling of the catalysts did not change its physico-chemical characteristic and the product distribution significantly. Table 4 shows the product distribution after a reaction time of 3 h.

It was seen, that the highest amount of HRTP (high retention time products) was registered using Beta(55). The camphene selectivity was found to be in an order: MCM-41(24) > amorphous > Beta(55), and the camphene/(camphene + limonene) selectivity was found to be: Beta(55) > MCM-41(24) ≈ amorphous. In the literature, similar experiments have been described with zeolites [11,12] (Table 5). Unfortunately, no detailed catalyst characterization was provided, for accurate comparison with our results. It was shown, that the overall conversion of alpha-pinene, as well as, the formation of camphene increased with an increase in acidity [11] and the transformation of limonene and alpha-pinene into heavy products was six times greater on mesoporous amorphous aluminosilicate than over dealuminated mordenite [13].

Table 5
Alpha-pinene isomerization over zeolites given in references [11–13]

Catalyst	BET (m^2/g)	Conversion of alpha-pinene (%)
H-MOR (6.99)	350	34.0[a]
D-MOR(7.70)	440	30.4[a]
D-MOR(29.7)	442	47.3[a]
D-MOR(49.2)	463	79.0[a]
D-MOR(66.4)	439	19.2[a]
D-MOR(186)	426	3.67[a]
Amorphous silica–alumina (SA)	120	98.9[a]
Catalyst		Conversion of alpha-pinene (%)
ZSM-5(35)		90.0[b]
ZSM-5(235)		43.0[b]
H-MOR		77.0[b]
HBeta(10)		75.0[c]

[a] The number in the brackets shows (Si/Al) bulk; reaction conditions: temperature—393 K, reaction duration—1 h, catalyst loading—17.2 (g α-pinene/g catalyst). D-MOR—dealuminated mordenite; (SA) contains 13 wt.% alumina.
[b] The number in the brackets shows (SiO_2/Al_2O_3 ratio), reaction conditions: temperature—373 K, reaction duration—5 h, catalyst loading—10.7.
[c] The number in the brackets shows (Si/Al ratio), outer surface dealuminated sample, reaction conditions: temperature—329 K, reaction duration—5 h, catalyst loading—0.45.

Based on the published data and our experimental data, it could be concluded that alpha-pinene isomerization is a complex reaction, in which zeolite framework irregularities, mesoporosity and acid site dispersion have a major influence. However, the acidity seemed to be the governing factor for alpha-pinene isomerization.

In our experiments, a Gaussian distribution is obtained regarding the time dependence of alpha-pinene conversion. The Gaussian distribution was usually caused by the difference in the strength of molecule adsorption in the transition state. The adsorption strength, on the other hand, was closely related to the electron density of the site. Using quantum-chemical calculations, useful information could be obtained about the reactions intermediate. In Fig. 4, two clusters with Brønsted sites are presented for the ZSM-5 zeolite. The clusters were optimized by the semi-empirical method INDO/1.

Clusters comprising a protonated α-pinene intermediate (Fig. 5) were simulated and optimized.

The relative energies of the optimized geometry, the charges of the sorbed C atom, Al atom and its environmental acidic oxygen atoms are compared in Table 6. As is seen from the data in the table, the protonation of alpha-pinene, which occurred in the transition states, was mostly favored in presence of Beta zeolite, as seen from the values of the relative substitution energy (ER). The latter was estimated as a difference between the energy of the α-pinene cluster and the initial zeolite cluster of the same geometry. More stable pinene intermediate complexes were formed on cluster "A" and on Beta type zeolite. The formation of the *p*-menthenyl cation was favored on the Beta and ZSM-5 samples, while on MCM-41 pinyl and isobornyl cations were energetically favored.

The measured angles in the ZSM-5 clusters varied significantly (107°–113°), revealing a significant tension in the transition state (most probably due to the dimensions of the alpha-pinene molecule), while the angles for Beta and MCM-41 are equal and about 109°. The differences suggest steric

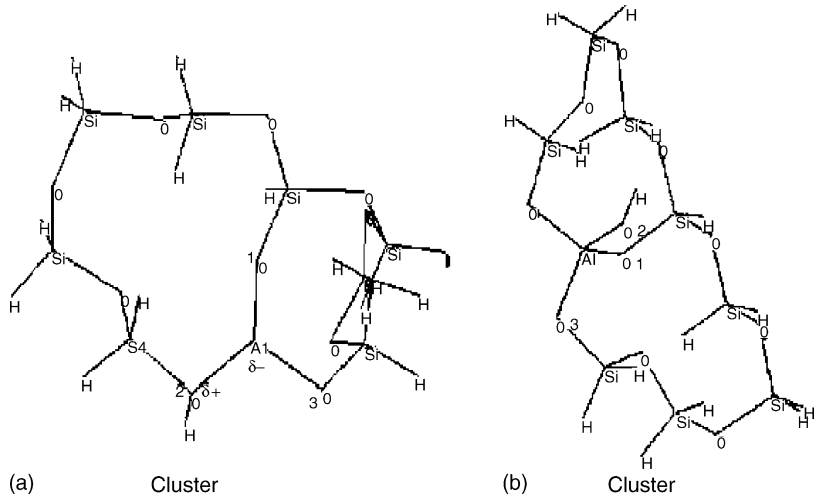

Fig. 4. Schematic presentation of equilibrium structure of ZSM-5 clusters.

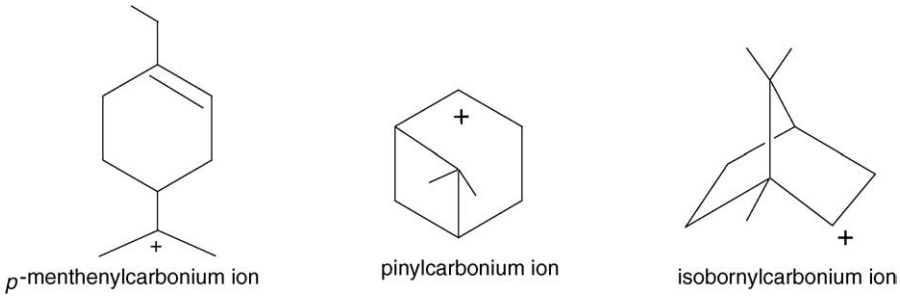

Fig. 5. Schematic presentation of α-pinene carbocations.

hindrance in the transition states over the different zeolites. Additional information for the cluster properties was gained by considering the atomic charge distribution. The positive charge of the Al-atom diminished in the order ZSM-5 > Beta > MCM-41. The positive charge of the Al-atom strongly effects the electron density of its neighboring oxygen atoms and the joined C atom. It is worth mentioning the negative charge of some Cads atoms which gives evidence for the strain in the transition state, so that cations could easily rearrange. The effect was more pronounced in the presence of Beta structure.

Table 6
Relative substitution energy (E_R) and atomic charges of equilibrium structures of the intermediate state

Models	E_R^a (kcal/mol)	Net atomic charges		
		Al-atom	C_{ads}^c	O_{acid}
Menthenyl_A_ZSM-5	−8360.4062	0.8308	0.182	−0.2961
Menthenyl_B_ZSM-5	−7673.6626	0.5779	0.048	−0.2039
Pinyl_A_ZSM-5	−9779.6465	0.3913	0.2052	−0.4155
Pinyl_B_ZSM-5	−9163.0293	0.4899	0.096	−0.2036
Isobornyl_A_ZSM-5	−9525.4736	0.4870	0.037	−0.1861
Isobornyl_B_ZSM-5	−9056.9258	0.5225	0.213	−0.2263
Menthenyl_A_Beta	−10506.6631	0.2492	−0.0536	−0.2022
Menthenyl_B_ Beta	−9909.2354	0.3878	0.1709	−0.2732
Pinyl_A_ Beta	−9680.3262	0.4238	−0.0350	−.04423
Pinyl_B_ Beta	−9266.1494	0.4506	−0.0245	−0.2458
Isobornyl_A_ Beta	−9831.4268	0.3652	0.0101	−0.4876
Isobornyl_B_ Beta	−9424.2383	0.4934	−0.1985	−0.4113
Menthenyl_A_MCM-41	−9149.4189	0.1025	−0.0118	−0.1403
Menthenyl_B_ MCM-41	−9062.7637	0.4467	0.1697	−0.2695
Pinyl_A_ MCM-41	−9271.5166	0.5137	0.0034	−0.2921
Pinyl_B_ MCM-41	−9490.6084	0.4296	0.0970	−0.1244
Isobornyl_A_ MCM-41	−9237.2988	0.4923	0.0919	−0.1653
Isobornyl_B_ MCM-41	−9473.1797	0.4514	−0.1387	−0.2366

4. Conclusions

Due to zeolite framework irregularities, the Brönsted sites are not unique. Its acid strength and dispersion were shown to be the governing factor for zeolite activity in the case of proton catalyzed reactions as methanol conversion and alpha-pinene isomerization. For the latter, a major effect was due to the existence of pores about 10–20 nm in size which provided easy access of the bulky alpha-pinene molecule to the acid site. The cluster approximation of the protonated zeolite site could be used for computation of transition state geometry and provided additional information in support of the experimental data.

Acknowledgements

Funding for this work from Turkish Scientific Research Council through Grant MISAG-Bulgaria 1 and from Bulgarian Academy of Sciences is gratefully acknowledged.

References

[1] C. Jia, P. Massiani, D. Barthomeuf, J. Chem. Soc. Faraday Trans. 89 (1993) 3659.
[2] C.P. Nicolaides, Appl. Catal. A: General 185 (1999) 211.
[3] R. Dimitrova, G. Gündüz, L. Dimitrov, T. Tsoncheva, S. Yilmaz, E.A. Urquieta-Gonzalez, J. Mol. Catal. A: Gen. 214 (2004) 265.
[4] Kiriesi, C. Flego, G. Pazzuconi, J. Phys. Chem. 98 (1994) 4624.
[5] M. Muller, G. Harvey, R. Prins, Micropor. Mesopor. Mater. 34 (2000) 135.
[6] J. Jancen, E. Creyghton, S. Njo, H. van Koningsveld, H. van Bekkum, Catal. Today 38 (1997) 205.
[7] G. Allahverdiev, D. Gündüz, Yu. Murzin, Ind. Eng. Chem. Res. 37 (1998) 2373.
[8] L. Grozona, N. Comelli, O. Massini, E. Ponzi, M. Ponzi, React. Kinet. Catal. Lett. 69 (2000) 271.
[9] F. Özkan, G. Gündüz, O. Akpolat, N. Beşün, D.Yu. Murzin, Chem. Eng. J. 91 (2003) 257.
[10] Y.M. Kr, D.Ch. Chintansinh, R.V. Jasra, J. Mol. Catal. A: Chem. 216 (2004) 51.
[11] De Stefanis, G. Perez, O. Ursini, A. Tomlinson, Appl. Catal. A:Gen. 132 (1995) 353.
[12] J.C. Van der Waal, H. van Bekkum, J.M. Vital, Mol. Catal. A: Chem. 105 (1996) 185.
[13] M. Lopez, F.J. Machado, K. Rodriguez, B. Mendez, M. Hagegawa, S. Pekerar, Appl. Catal. A: Gen. 173 (1998) 75.
[14] K. Genske, H. Bornholdt, Lechert, Stud. Surf. Sci. Catal. 117 (1998) 421.
[15] Q. Zhao, J. Huo, B.F.C. Feng, G.D. Stucky, J. Am. Chem. Soc. 120 (1998) 6024.
[16] X.S. Zhao, G.Q. (Max) Lu, G.J. Millar, Ind. Eng. Chem. Res. 35 (1996) 2075.